

Supporting Information

Boundary Layer Effect on Solvent Evaporation during Perovskite Film

Drying by Multi-flow Air Knife

Li-Li Gao, Ke-Jie Zhang, Chen Ni and Guan-Jun Yang*

School of Materials Science and Engineering, Xi'an Jiaotong University, Xi'an, Shaanxi 710049, P.R. China

* E-mail: ygj@mail.xjtu.edu.cn

Experimental section

Materials preparation

Lead iodide (PbI_2 , 99.99%), N,N-dimethylformamide (DMF, 99.8%), iodine methylamine ($\text{CH}_3\text{NH}_3\text{I}$) were purchased from Xi'an Polymer Light Technology Corp., and used as received. Titanium dioxide precursor solvent was synthesized following the reported procedure.¹ Spiro-MeOTAD solution was prepared according to the report.² It was prepared by dissolving 72.3 mg of spiro-MeOTAD in 1 ml of chlorobenzene, to which 28.8 μl of 4-tert-butylpyridine and 17.5 μl of lithiumbis(trifluoromethanesulfonyl)imide (Li-TFSI) solution (520 mg Li-TFSI in 1 ml acetonitrile, Sigma-Aldrich, 99.8%) were added.

Perovskite film fabrication

The perovskite precursor solution was composed of PbI_2 and $\text{CH}_3\text{NH}_3\text{I}$ at a molar ratio of 1:1, which dissolved in DMF solvent at 70 °C and stirred for 12 h. An appropriate amount of perovskite precursor solution was dropped on the TiO_2 -coated FTO surface and spun at 5000 rpm for 6 s, a light yellow liquid perovskite precursor film of $\sim 3 \mu\text{m}$ in thickness was obtained. Subsequently, MAK swept across the solution film at various air flow rates and air temperatures. In this study, we adopted the flow rate values of 50, 150, 250 and 350 L min^{-1} , using several different air temperatures, 20, 50, 100, 150 °C. The dried films were annealed for 10 min at 100 °C on a hot plate.

Perovskite Solar Cell Fabrication

Devices were fabricated on Fluorine-doped tin oxide (FTO) coated glass (Pilkington, $15 \Omega \text{ sq}^{-1}$). The FTO substrates were cut into 25 mm \times 25 mm pieces and rinsed sequentially with acetone, ethyl alcohol, and deionized water in an ultrasonic bath for 10 min, and then blow dried by nitrogen. The FTO substrates were treated with ozone and ultraviolet light for 15 min for increasing wettability. TiO_2 was deposited by spin coating at 4500 rpm for 30 s as the electron transport layer of compact, and sintered at 500 °C for 30 min. The dense TiO_2 layer was $\sim 50 \text{ nm}$ thick. A compact 300 nm thick perovskite film, as the light absorption layer, was deposited by MAK method on the TiO_2 layer. All above steps were conducted under ambient conditions at the temperature of 20 °C and humidity of 30%. About 20 μL spiro-OMeTAD solution was spin coated on perovskite films at 4000 rpm for 30 s. Then it was left overnight to allow for the spiro-OMeTAD doping via oxidation in a drying box with humidity of 13%. Finally, an 80-

nm-thick Au layer was deposited by thermal evaporation under vacuum of 4×10^{-4} Pa. The finished device was stored in a N₂-purged glovebox (<0.1 ppm O₂ and H₂O) before measurement.

Measurement and Characterization

The XRD patterns of the FTO substrate and perovskite film were obtained with a D8 Advance X-ray diffractometer with Cu K_α radiation. All samples were scanned from 10° to 60° with a step size of 0.2°. The absorption spectra of the perovskite films were measured with a U-3010 spectrophotometer. The surface morphologies of the perovskite films were examined using SEM (VEGA II-XMU, TESCAN, Czech Republic). AFM (Veeco dilnnova, Bruker, America) was used to examine the surface profile and roughness. J–V curves of the perovskite solar cells were measured using a Keithley 2400 source-measure unit under the illumination of simulated sunlight, provided by a 450 W Class AAA solar simulator equipped with a filtered Xe lamp, (AM 1.5G, 100 mW cm⁻², Sol3A, Oriel Instruments). The output light intensity was calibrated using a single-crystal silicon photovoltaic cell as the reference (91150V, Oriel Instruments). The cells were measured with a non-reflective metal mask covering areas of 1 and 0.1 cm² to receive sunlight and avoid light scattering through the edges. The current densities of the devices were measured by biasing the devices at maximum power point for 150 s, and then calculating the steady-state power conversion efficiency by multiply steady-state current densities and maximum biasing. IPCE spectra of the device was tested in air without bias light by using a Qtest Station 1000ADX system (Growntech, Inc.). The illumination spot size was slightly smaller than the active area of the test cells. IPCE photocurrents were recorded under short-circuit conditions using a Keithley 2400 source meter. The monochromatic photon flux was quantified by means of a calibrated silicon photodiode. Electrochemical impedance spectroscopy (EIS) analysis was conducted on a ZAHNER ENNIUM Electrochemical Workstation.

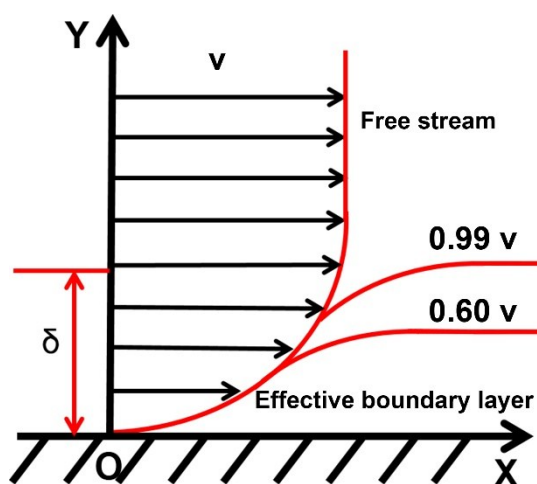


Fig. S1 Schematic diagram of the boundary layer.

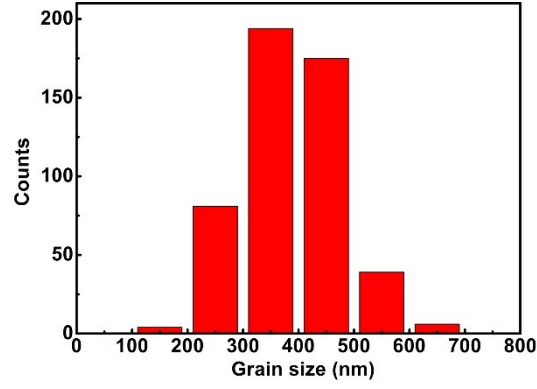


Fig. S2 Grain size distribution of perovskite grains.

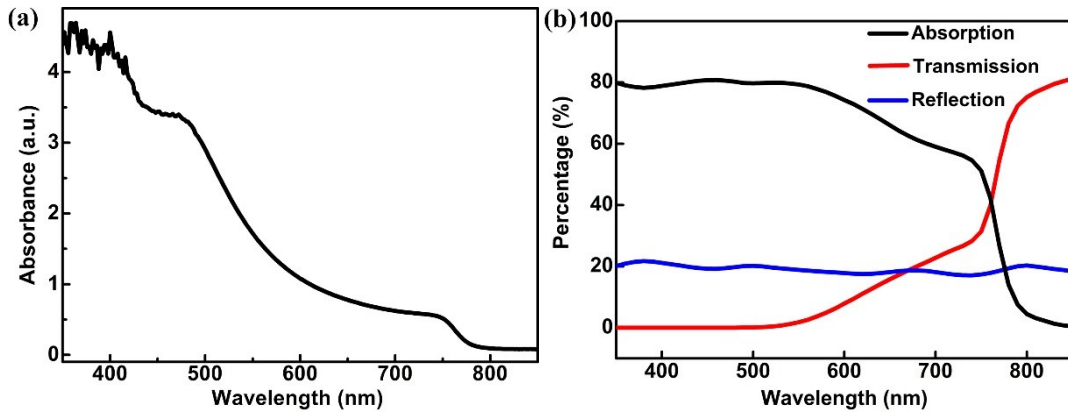


Fig. S3 (a) Absorbance spectrum of perovskite film dried by multi-flow air knife, (b) absorbance, transmission, and reflection percentage of perovskite film dried by multi-flow air knife.

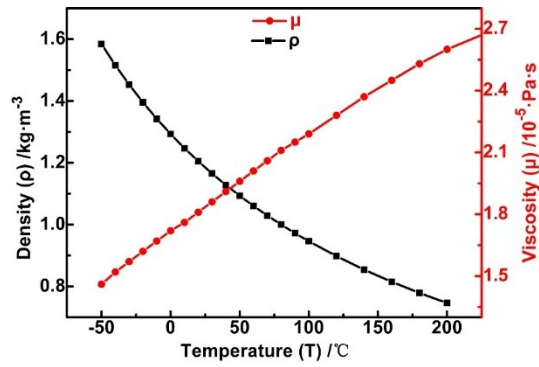


Fig. S4 Air density and viscosity variation tendency along temperature increasing.

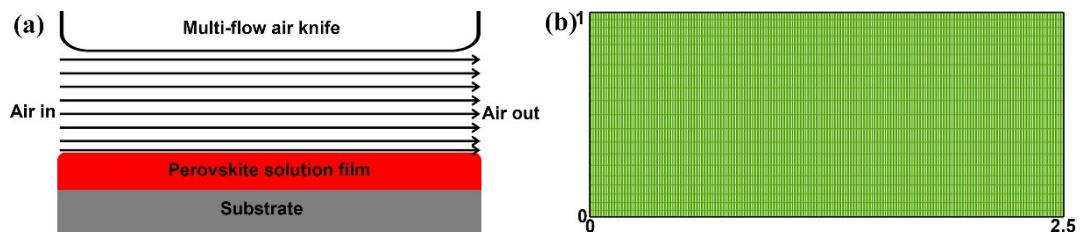


Fig. S5 Schematic diagram of one unit multi-flow air knife drying (a), simulation mesh (b).

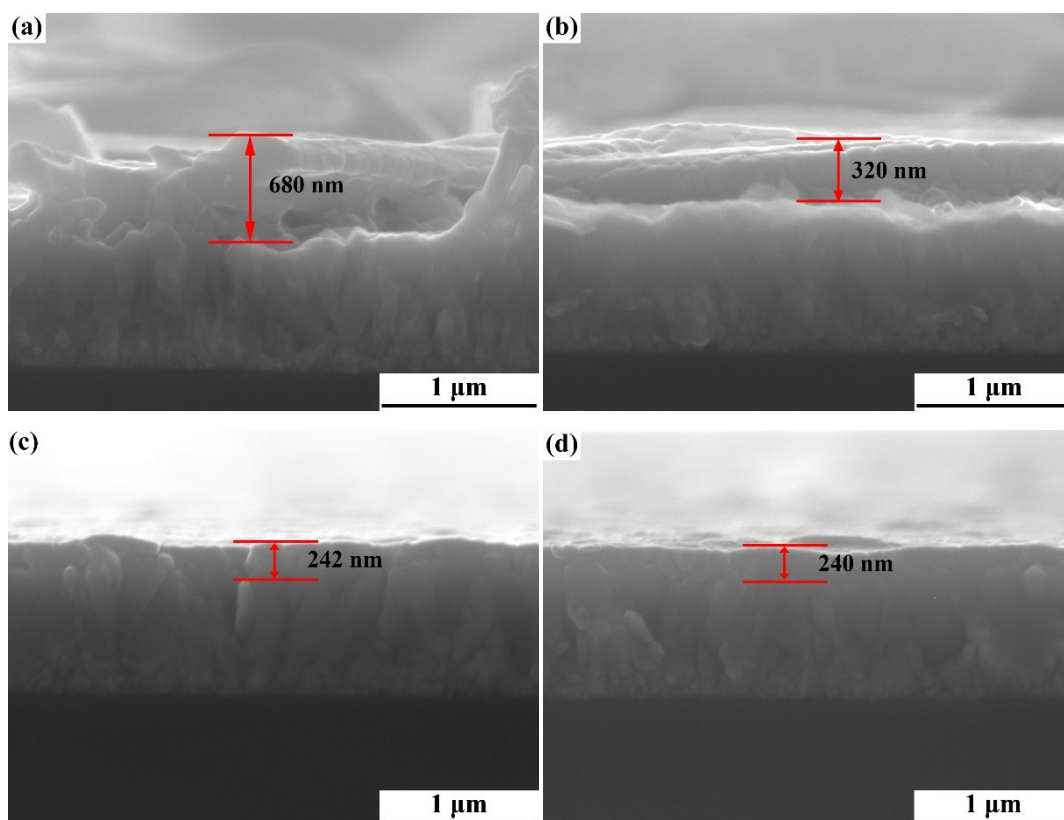


Fig. S6 The cross sectional images of perovskite film dried at 20°C with varied air flow velocities, (a) 6.55 m/s (50 L min⁻¹); (b) 19.66 m/s (150 L min⁻¹); (c) 32.77 m/s (250 L min⁻¹); (d) 45.87 m/s (350 L min⁻¹).

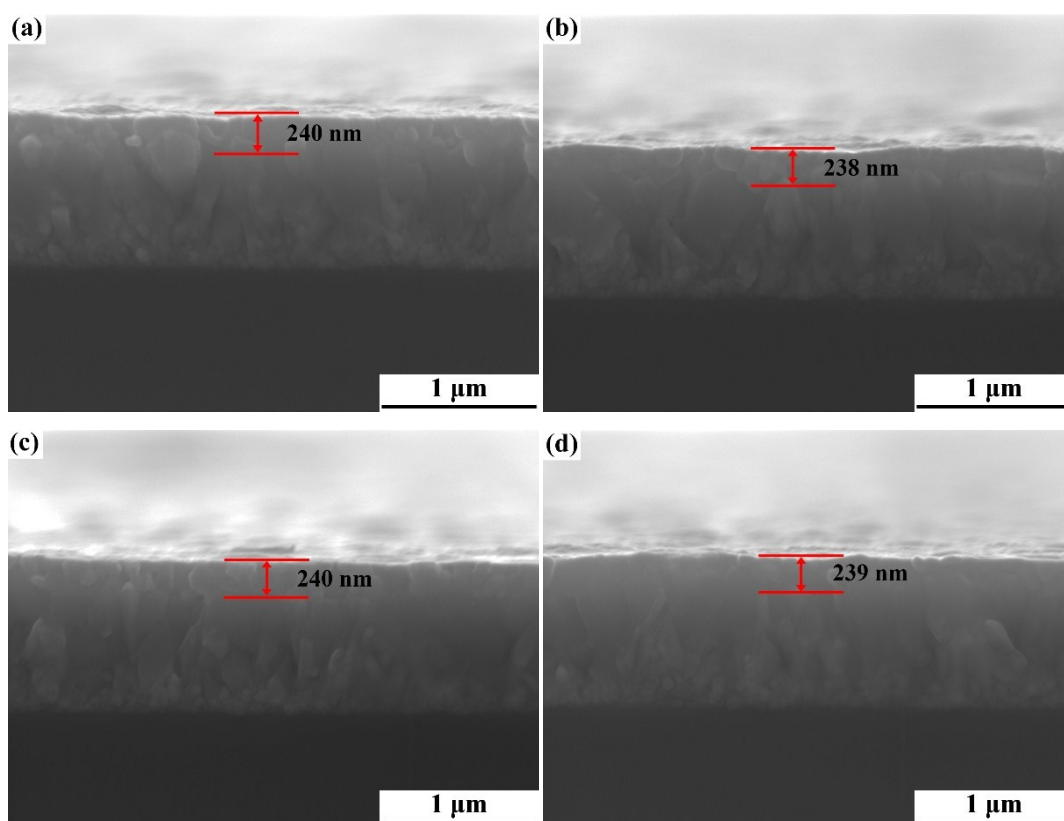


Fig. S7 The cross sectional images of perovskite film dried at 350 L min^{-1} with different air-flow temperatures, (a) 20°C ; (b) 50°C ; (c) 100°C ; (d) 150°C .

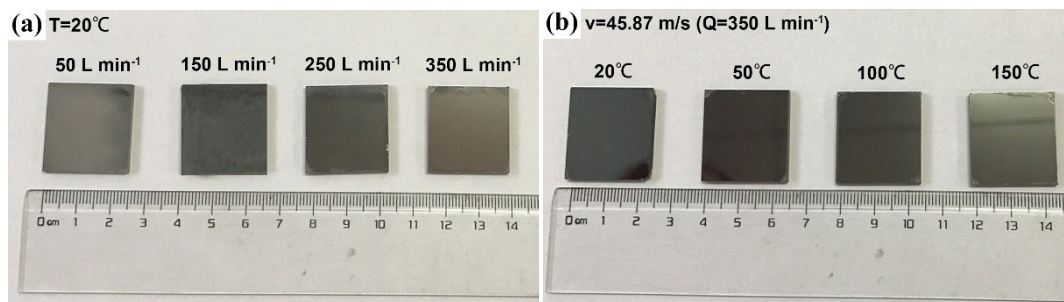


Fig. S8 Photograph of perovskite films dried by air flow at different parameters.

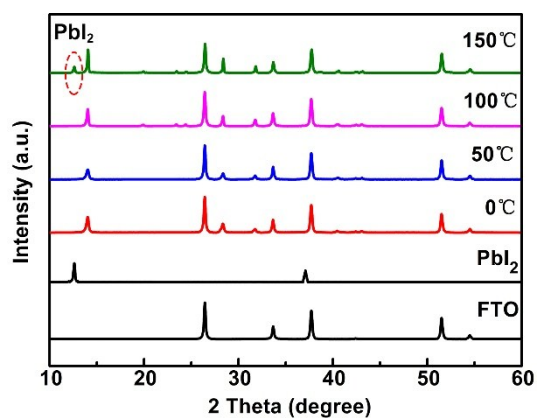


Fig. S9 XRD patterns of the MAK dried $\text{CH}_3\text{NH}_3\text{PbI}_3$ film annealing at different temperatures.

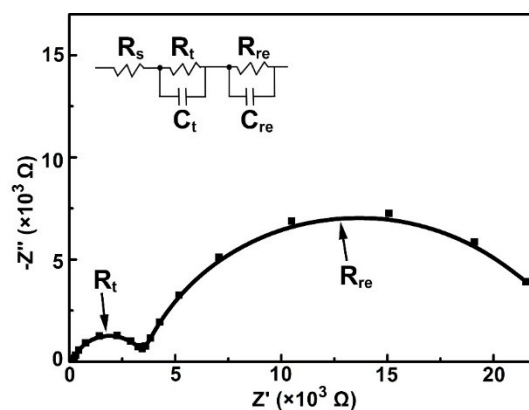


Fig. S10 The electrochemical impedance spectrum of the device at a forward bias 1.0 V under illumination.

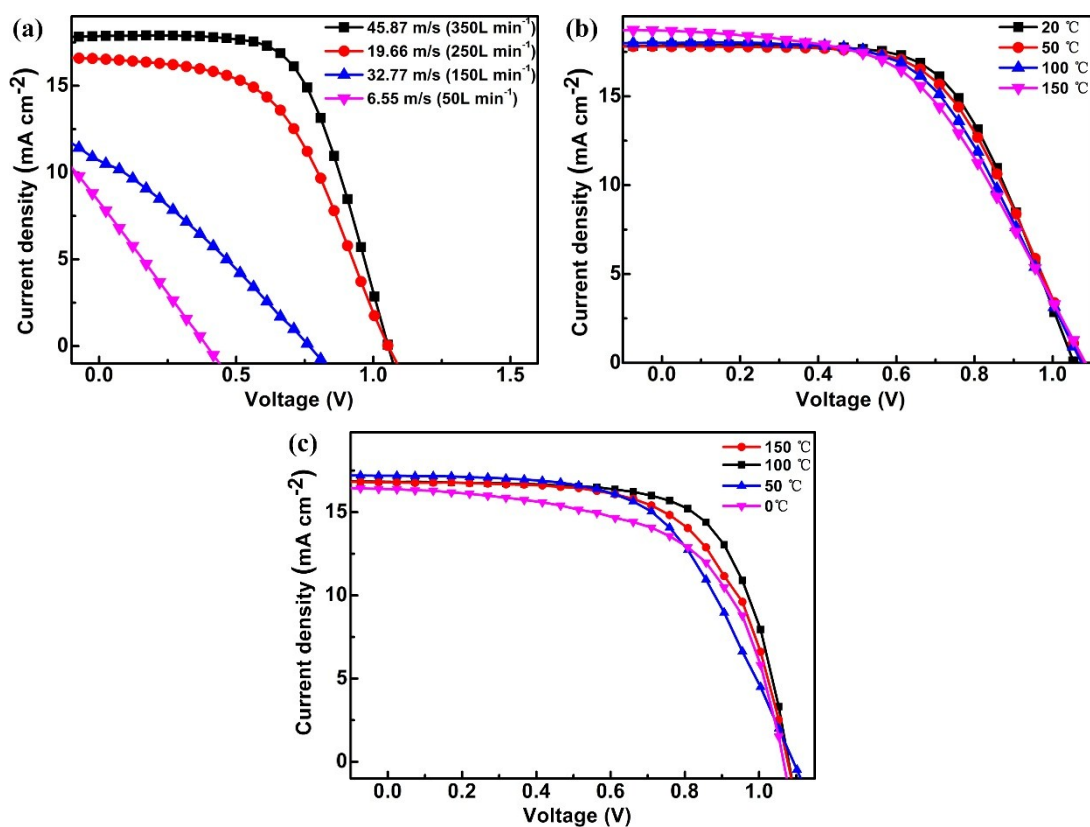


Fig. S11 J-V curves of the device with different condition perovskite films, (a) films dried by various air velocities at $20\text{ }^{\circ}\text{C}$, (b) films dried by various air temperatures at 45.87 m/s (350 L min^{-1}), (c) films annealed at different temperatures for 10 min.

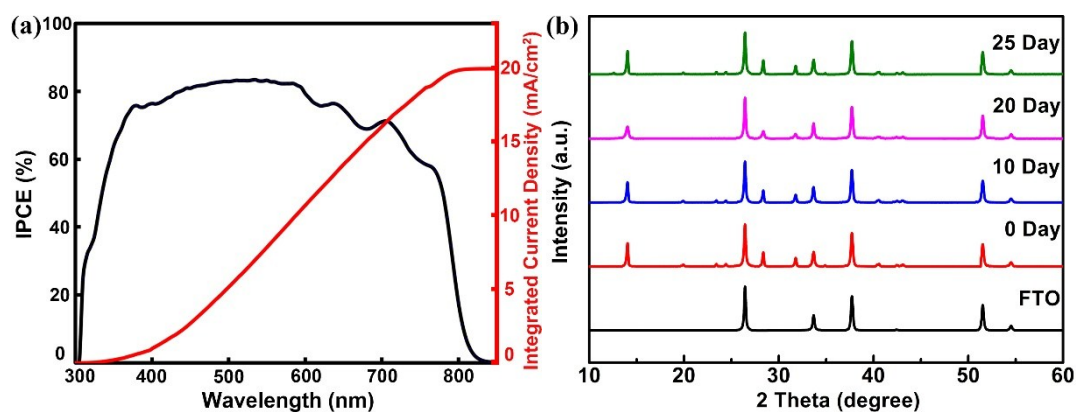


Fig. S12 (a) IPCE spectra of the device with active area of 0.1 cm^2 , (b) XRD patterns of the MAK dried perovskite film measured at different moment.

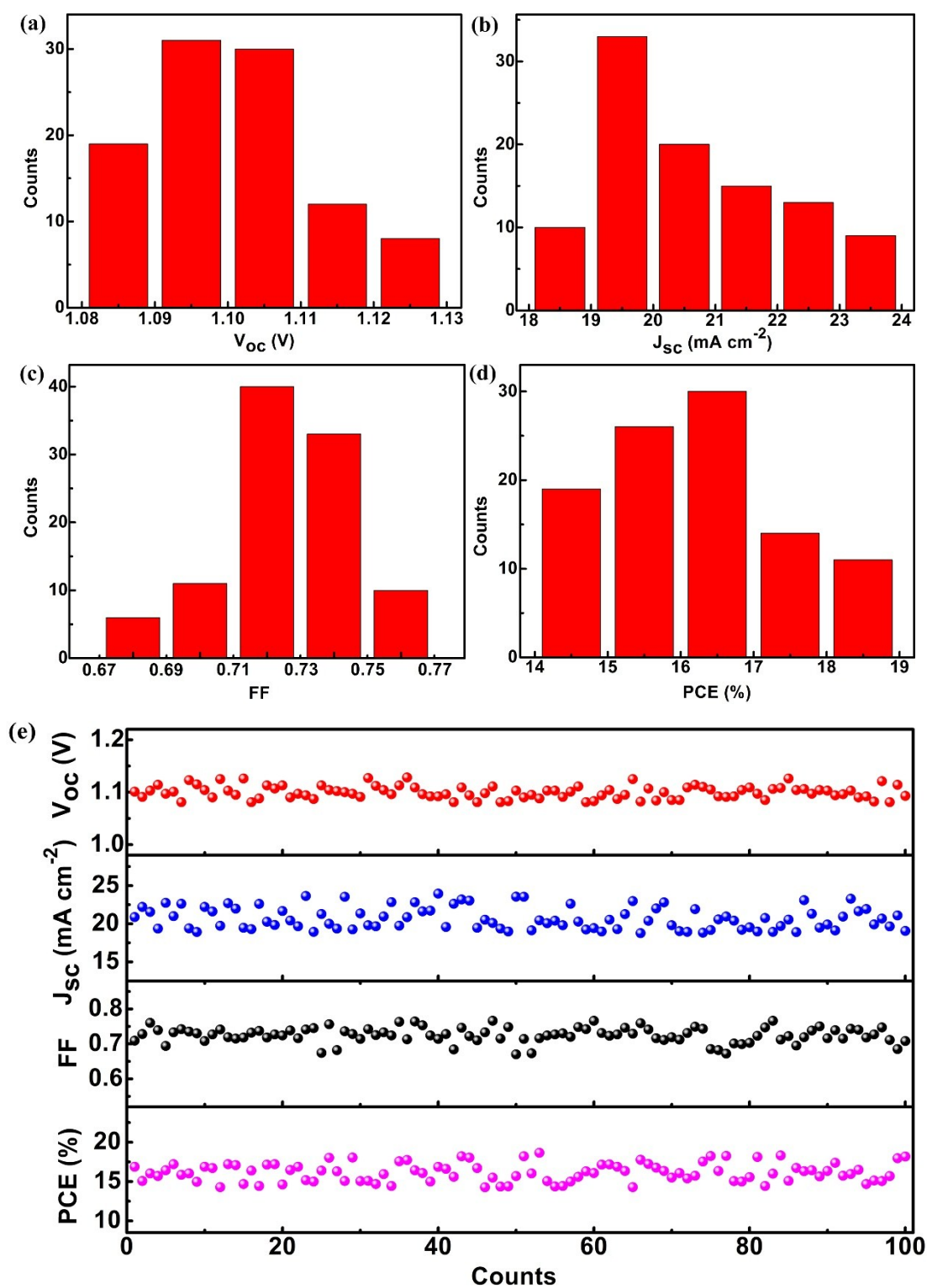


Fig. S13 The performances statistics of 100 devices, (a) V_{OC} , (b) J_{SC} , (c) FF, (d) PCE, (e) every parameter value

distribution V_{OC} , J_{SC} , FF and PCE.

Table S1 Boundary layer thickness with varied air temperatures and varied air velocities. Here, $L=d=0.025$ m. All air velocity is consisted with an air flow, which can be tuned mechanically.

T (°C)	ρ (kg/m ³)	η ($\times 10^{-5}$ Pa·s)	v (m/s)	Q (L min ⁻¹)	δ (μ m)
20°C	1.205	1.81	6.55	50	239.4
20°C	1.205	1.81	19.66	150	138.2
20°C	1.205	1.81	32.77	250	107.0
20°C	1.205	1.81	45.87	350	90.5
50°C	1.093	1.96	6.55	50	261.6
50°C	1.093	1.96	19.66	150	151.0
50°C	1.093	1.96	32.77	250	116.9
50°C	1.093	1.96	45.87	350	98.9
100°C	0.946	2.19	6.55	50	297.3
100°C	0.946	2.19	19.66	150	171.6
100°C	0.946	2.19	32.77	250	132.9
100°C	0.946	2.19	45.87	350	112.3
150°C	0.835	2.41	6.55	50	331.9
150°C	0.835	2.41	19.66	150	191.6
150°C	0.835	2.41	32.77	250	148.4
150°C	0.835	2.41	45.87	350	125.4

1. Li, N.; Dong, H.; Dong, H.; Li, J.; Li, W.; Niu, G.; Guo, X.; Wu, Z.; Wang, L., Multifunctional perovskite capping layers in hybrid solar cells. *J Mater Chem A* **2014**, 2 (36), 14973.
2. Im, J. H.; Jang, I. H.; Pellet, N.; Gratzel, M.; Park, N. G., Growth of CH₃NH₃PbI₃ cuboids with controlled size for high-efficiency perovskite solar cells. *Nat Nanotechnol* **2014**, 9 (11), 927-932.